nature biotechnology

Cell-surface markers for the isolation of pancreatic cell types derived from human embryonic stem cells

Olivia G Kelly, Man Yin Chan, Laura A Martinson, Kuniko Kadoya, Traci M Ostertag, Kelly G Ross, Mike Richardson, Melissa K Carpenter, Kevin A D'Amour, Evert Kroon, Mark Moorman, Emmanuel E Baetge & Anne G Bang

Using a flow cytometry–based screen of commercial antibodies, we have identified cell-surface markers for the separation of pancreatic cell types derived from human embryonic stem (hES) cells. We show enrichment of pancreatic endoderm cells using CD142 and of endocrine cells using CD200 and CD318. After transplantation into mice, enriched pancreatic endoderm cells give rise to all the pancreatic lineages, including functional insulin-producing cells, demonstrating that they are pancreatic progenitors. In contrast, implanted, enriched polyhormonal endocrine cells principally give rise to glucagon cells. These antibodies will aid investigations that use pancreatic cells generated from pluripotent stem cells to study diabetes and pancreas biology.

The limited supply of human islets available for diabetes cell therapies has focused attention on using hES cells as a potential renewable source for beta cells[1,2]. Previously, we demonstrated the directed differentiation of hES cells into pancreatic lineages[3,4]. *In vitro*, differentiated hES cells secreted insulin in response to various stimuli but not in response to glucose; however, after implantation into mice, they generated glucose-responsive, insulin-secreting cells[4]. The hES cell–derived pancreatic cell cultures consisted of a mixture of cell types, including pancreatic endoderm (PE) cells and polyhormonal endocrine cells. In the present study, we identified CD142 as a surface marker for PE cells and CD200 or CD318 as surface markers for endocrine cells, which permitted the isolation of these different cell populations for functional analyses. These analyses demonstrated that PE cells, but not polyhormonal endocrine cells, are pancreatic progenitors that give rise to islets with glucose-responsive insulin-secreting cells *in vivo*. Surface markers to monitor cell subsets will be valuable for establishing and improving conditions for differentiating pluripotent stem cells into pancreatic cells. Also, the ability to isolate pancreatic cell types from stem cell–derived cultures and tissues will be useful for the development of diabetes therapies and for addressing fundamental questions about pancreas biology and disease[5,6].

RESULTS

Identification of pancreatic cell-surface markers

We used flow cytometry analysis to assess the cellular compositions of pancreatic cell cultures differentiated from hES cells with our multistep protocol[3,4] (**Supplementary Fig. 1a**). Hormone-expressing cells, including insulin$^+$ cells, were positive for the endocrine marker chromogranin A[7] (encoded by *CHGA*; **Supplementary Fig. 1b**, **Supplementary Table 1** and data not shown), and PE cells were CHGA$^-$/NKX6.1$^+$ and PDX1$^+$[1,8] (**Supplementary Fig. 1c**), consistent with our prior immunocytochemical observations[3,4]. The proportions of distinct pancreatic cell types varied among cultures and among different hES cell lines (**Supplementary Fig. 1d**; CyT49 hES cell–derived cultures, n = 14: median = 25.4% CHGA$^+$, 45.7% PE; CyT203 hES cell–derived cultures n = 5: median = 21.6% CHGA$^+$, 25.7% PE; MEL1 hES cell–derived cultures n = 6: median = 1.08% CHGA$^+$, 6.25% PE). We designed a flow cytometry–based strategy to screen commercial antibodies against cell-surface proteins with the goal of identifying reagents that could distinguish these pancreatic cell subsets (**Supplementary Fig. 2**).

The screen identified three promising cell-surface markers: CD200 and CD318 for endocrine cells and CD142 for PE cells. We further explored these markers in CyT49 hES cell–derived cultures. The majority of CHGA$^+$ endocrine cells in the cultures were contained within either a CD200^{bright} or a CD318^{bright} population, with CD200 being more restricted to endocrine cells, particularly on day 12 (**Fig. 1a**,**b**). In contrast, only a minor population of CD142^{bright}/CHGA$^+$ cells was observed (**Fig. 1c**). Consistent with this pattern, co-staining with CD142 and CD200 revealed very little overlap with only a small population of double-positive CD200^{bright}/CD142^{bright} cells (**Fig. 1d**). Instead, the CD142^{bright} population consisted principally of CHGA$^-$/NKX6.1$^+$ PE cells, although some CHGA$^-$/NKX6.1$^-$ cells were also present (**Fig. 1e**). The proportion of total CHGA$^-$/NKX6.1$^+$ PE cells that were not CD142^{bright} was variable among cultures. The CD142^{bright}/NKX6.1$^+$ PE cells were also PDX1$^+$ (**Supplementary Fig. 3**). At an earlier stage of differentiation, on day 10, few CD142^{bright} and few PE cells were present (**Fig. 1e**). These data demonstrate that CD142 primarily demarcated NKX6.1$^+$/PDX1$^+$ PE cells after the onset of NKX6.1 protein expression. In accordance with the flow cytometry analyses, we mostly found CD142 immunostaining on the surface of PE cells and CD200 immunostaining on the surface of endocrine cells, in intact cultures (**Fig. 1f**). Also, in the human adult

ViaCyte, Inc. (formerly Novocell, Inc.), San Diego, California, USA. Correspondence should be addressed to O.G.K. (okelly@viacyte.com).

Received 17 May; accepted 5 July; published online 31 July 2011; doi:10.1038/nbt.1931

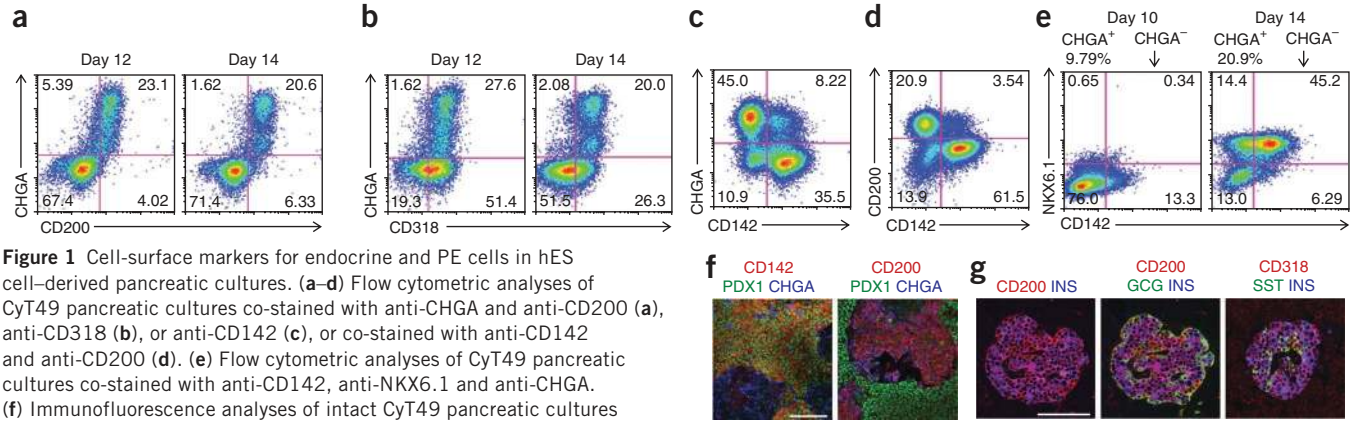

Figure 1 Cell-surface markers for endocrine and PE cells in hES cell–derived pancreatic cultures. (**a**–**d**) Flow cytometric analyses of CyT49 pancreatic cultures co-stained with anti-CHGA and anti-CD200 (**a**), anti-CD318 (**b**), or anti-CD142 (**c**), or co-stained with anti-CD142 and anti-CD200 (**d**). (**e**) Flow cytometric analyses of CyT49 pancreatic cultures co-stained with anti-CD142, anti-NKX6.1 and anti-CHGA. (**f**) Immunofluorescence analyses of intact CyT49 pancreatic cultures with anti-PDX1 (green), anti-CHGA (blue), anti-CD142 (red) and anti-CD200 (red). Scale bar, 100 μm. (**g**) Immunofluorescence analyses of adult human pancreas with anti-CD318 (red), anti-CD200 (red), anti-SST (green), anti-GCG (green) and anti-INS (blue). Scale bar, 100 μm. CHGA, chromogranin A; INS, insulin; GCG, glucagon; SST, somatostatin.

pancreas, CD200 and CD318 were present on the membrane of islet cells, and CD318 was weakly detected on exocrine cells (**Fig. 1g**).

To explore the broad utility of these cell-surface markers, we examined other hES cell lines (**Supplementary Fig. 4**). Similar pancreatic cell populations were demarcated by all three cell-surface markers in CyT203 hES cell–derived cultures, although in some cases CD318 was expressed on a larger proportion of CHGA$^-$ cells (**Supplementary Fig. 4a**–**e** and **Supplementary Table 1**). In MEL1 hES cell–derived cultures, the small populations of PE and endocrine cells were demarcated by CD142, or CD200 and CD318, respectively (**Supplementary Fig. 4g**–**i**). Similarly, in an atypically poor pancreatic differentiation of a CyT49 culture, CD142 demarcated the minor PE population (**Supplementary Fig. 4f**). In these cultures with low PE production, however, the CHGA$^-$/NKX6.1$^-$ cells constituted a larger proportion of the CD142^{bright} population. Together these data show that antibodies to CD142, CD200 and CD318 can be used to monitor pancreatic cell subsets in cultures derived from three different hES cell lines that differentiate to PE and endocrine cells with varying efficiencies.

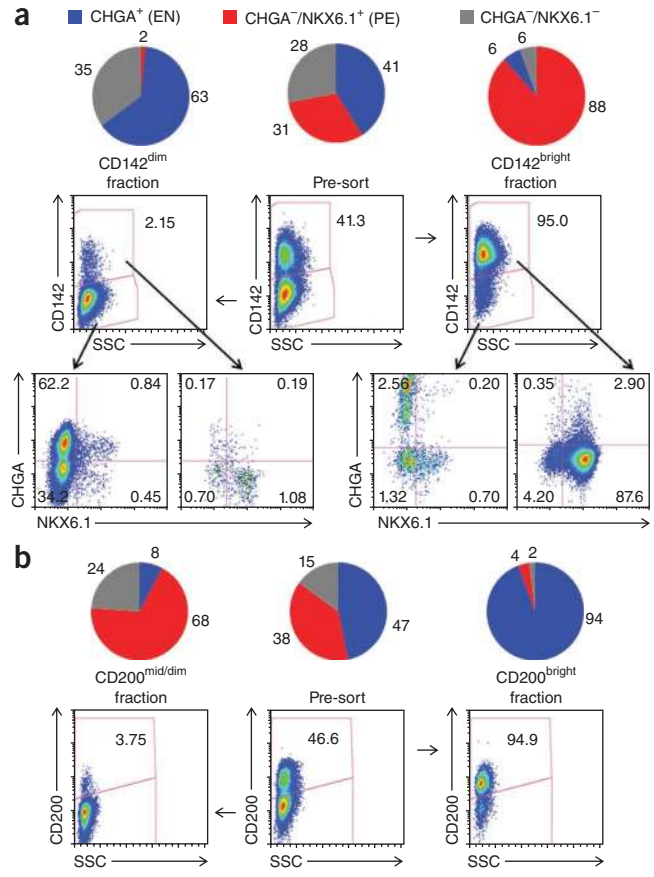

Figure 2 FACS isolation of CD142 and CD200 cell subsets from hES cell–derived pancreatic cultures. (**a**,**b**) Representative CD142 (**a**) and CD200 (**b**) FACS experiments of CyT49 differentiated cultures showing cellular compositions in the pre-sort population and isolated fractions as assessed by anti-CHGA and anti-NKX6.1 co-staining. Cellular compositions are represented as pie charts with CHGA$^+$ endocrine cells (EN, blue), CHGA$^-$/NKX6.1$^+$ PE cells (red) and CHGA$^-$/NKX6.1$^-$ cells (gray). CHGA, chromogranin A; SSC, side scatter.

Separation of pancreatic cell types with cell-surface markers

We next performed cell separation experiments using fluorescence-activated cell sorting (FACS; CD142, $n = 2$; CD200, $n = 2$). In a representative CD142 FACS experiment, we isolated a CD142^{bright} fraction (95% CD142^{bright} cells) that consisted principally of PE cells (88%) with a small percentage of CHGA$^+$ cells (6%) (**Fig. 2a**). Conversely, in the CD142^{dim} fraction (2.15% CD142^{bright} cells), the PE cells (2%) were largely excluded, resulting in a remaining mixture of CHGA$^+$ cells and CHGA$^-$/NKX6.1$^-$ cells. We similarly isolated fractions either enriched in (94.9%) or depleted of (3.75%) CD200^{bright} cells (**Fig. 2b**). The CD200^{bright} fraction primarily contained CHGA$^+$ cells (94%) with only 4% PE cells. In contrast, the CD200$^{mid/dim}$ fraction was depleted of CHGA$^+$ cells (8%), instead consisting mainly of PE cells and CHGA$^-$/NKX6.1$^-$ cells. Thus, we were able to isolate populations highly enriched in either PE cells with CD142 or in endocrine cells with CD200. Although such populations will be useful for molecular profiling analyses, we were not able to obtain a sufficient number of viable cells using FACS to perform transplantation experiments.

As an alternative to FACS, we investigated immuno-magnetic cell separation because it is gentler and because a large number of cells can be isolated at once in a reasonable time frame. With immuno-magnetic cell separations of CyT49 hES cell–derived cultures, we could achieve in some bound fractions enrichment of CD142^{bright} cells (90.7% ± 4.32%, $n = 5$) and CHGA$^-$/NKX6.1$^+$ PE cells (81.6% ± 7.66%, $n = 3$) and depletion of CHGA$^+$ cells (6.00% ± 1.81%, $n = 5$) similar to those obtained with FACS (**Fig. 3a** and **Table 1**). However, many CD142^{bright}

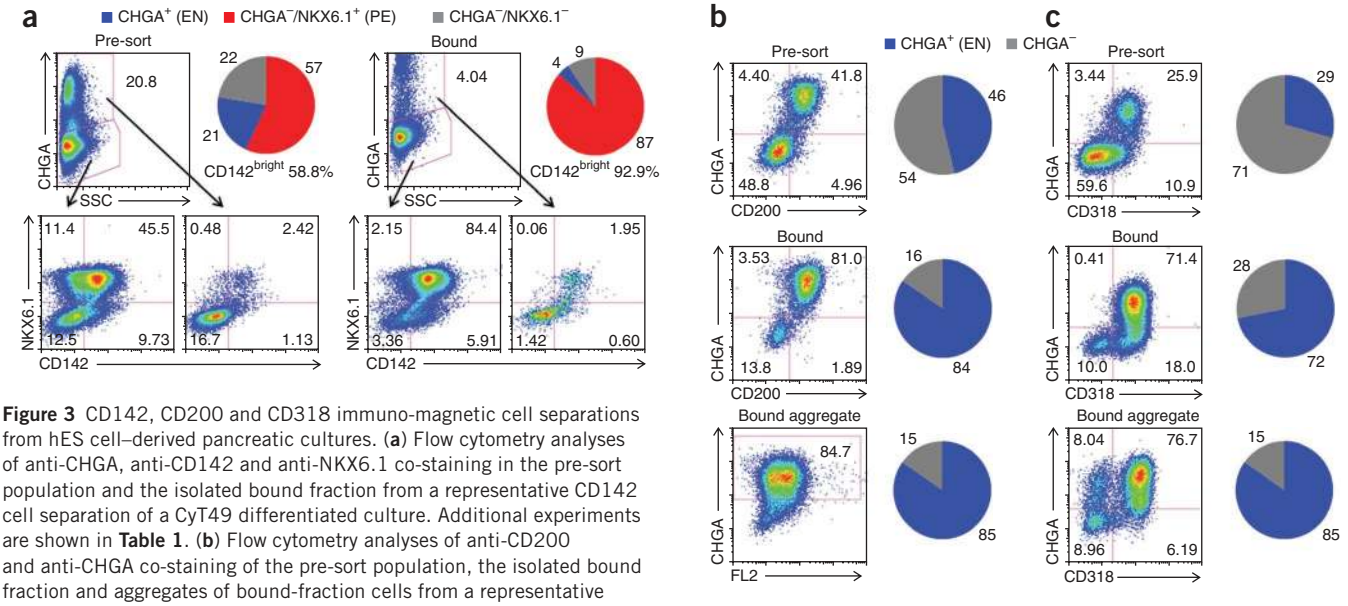

Figure 3 CD142, CD200 and CD318 immuno-magnetic cell separations from hES cell–derived pancreatic cultures. (**a**) Flow cytometry analyses of anti-CHGA, anti-CD142 and anti-NKX6.1 co-staining in the pre-sort population and the isolated bound fraction from a representative CD142 cell separation of a CyT49 differentiated culture. Additional experiments are shown in **Table 1**. (**b**) Flow cytometry analyses of anti-CD200 and anti-CHGA co-staining of the pre-sort population, the isolated bound fraction and aggregates of bound-fraction cells from a representative CD200 cell separation of a CyT49 differentiated culture. In this experiment the bound aggregate was not restained with CD200 (FL2). Additional experiments are shown in **Supplementary Table 1**. (**c**) Flow cytometry analyses of anti-CD318 and anti-CHGA co-staining of the pre-sort population, the isolated bound fraction and aggregates of bound-fraction cells from a representative CD318 cell separation of a CyT49 differentiated culture. Additional experiments are shown in **Supplementary Table 1**. Cellular compositions are represented as pie charts with CHGA$^+$ endocrine cells (EN, blue), CHGA$^-$/NKX6.1$^+$ PE cells (red), and CHGA$^-$/NKX6.1$^-$ cells (gray) or CHGA$^-$ cells (gray). CHGA, chromogranin A; SSC, side scatter.

cells were lost in the flow-through fraction. In a CyT49 cell separation in which the pre-sort culture contained a low percentage of CD142^{bright} cells (13.4%) and PE cells (6.60%), the bound fraction exhibited a lower level of purity, but nonetheless a substantial enrichment of CD142^{bright} cells (61.6%) and PE cells (48.7%) was observed (**Table 1**, experiment 6). Likewise, in pancreatic cell cultures derived from MEL1 hES cells, we also obtained a substantial enrichment in CD142^{bright} cells (74.9% ± 8.17%, n = 3) and CHGA$^-$/NKX6.1$^+$ PE cells (56.7%, n = 2) in the bound fraction despite the low production of CD142^{bright} cells (15.0% ± 11.2%, n = 3) and PE cells (5.37%, n = 2) in the pre-sort cultures (**Table 1**).

We also carried out immuno-magnetic cell separation experiments with CD200 and CD318 (**Fig. 3b**,**c** and **Supplementary Table 1**). The extent of enrichment of CHGA$^+$ endocrine cells in the bound fraction and depletion in the flow-through fraction was variable, depending upon the number of target cells in the initial pre-sort population and in the case of CD318, marker specificity. Nonetheless, in some cell isolations >84% CHGA$^+$ cells could be attained in the CD200-bound or CD318-bound fractions. Enrichment of insulin$^+$ cells in the bound fraction was observed as well (**Supplementary Table 1**). Quantitative PCR (qPCR) analyses of the expression of the endocrine markers *NKX2.2*, insulin (encoded by *INS*), and glucagon (encoded by *GCG*) in CD200 cell subsets demonstrated an increase in the bound fraction and a decrease in the flow-through fraction relative to the pre-sort population (**Supplementary Fig. 5**).

Because the three-dimensional structure of islets is important for their optimal function, we employed a rotational culture method to reaggregate the enriched endocrine cells into multicellular clusters[9]. Before our identification of CD200 and CD318, we initially developed this method using CD56 immuno-magnetic cell separations[10]. Whereas CHGA$^+$ endocrine cells were only partially enriched in the CD56-bound fraction (n = 4, pre-sort 24.0% ± 7.00%; bound 38.1% ± 8.88%), aggregation of bound-fraction cells resulted in a further enrichment in CHGA$^+$ cells (n = 4, 85.5% ± 5.55%), many of which were insulin and glucagon immunoreactive (**Supplementary Fig. 6**). Even reaggregation of dissociated cells that had not been sorted yielded enriched CHGA$^+$ endocrine aggregates (72.9%, n = 2; **Supplementary Fig. 6a**). Similarly, reaggregation of the CD200-bound- and CD318-bound-fraction cells generally resulted in further endocrine enrichment (**Fig. 3b**,**c** and **Supplementary Table 1**). However, as we did not always observe efficient endocrine enrichment with reaggregation, we postulated that the cellular composition of the CHGA$^-$ population was likely an important factor in determining the level of enrichment; as described further below, this observation may be related to the selective exclusion of PE cells, but not other unknown cell types, in the CHGA$^-$ population.

Developmental potential of endocrine cell–enriched population

Next we assessed the developmental potential of isolated polyhormonal endocrine cells or PE cells after implantation on Gelfoam sponges into the epididymal fat pads of severe combined immunodeficient–beige mice[4]. Aggregates were generated by rotational culture of dissociated cells, as discussed above, or through processing of intact cultures with a tissue chopper[4].

Explanted grafts of unenriched cells or C318-enriched endocrine cells were analyzed with immunofluorescence at various time points after engraftment (**Fig. 4**, n = 1–2 mice per time point). Before transplantation, the unenriched population contained 39.2% CHGA$^+$ cells, whereas the aggregated CD318-enriched population contained 92.3% CHGA$^+$ cells (**Supplementary Table 1**, experiment 7). Moreover, the CD318-enriched population was largely depleted of NKX6.1$^+$ cells (2.6%). Three weeks after transplant, both unenriched and CD318-enriched explants exhibited many cells expressing various combinations of insulin, glucagon and somatostatin as well as some expressing a single hormone (**Fig. 4a–d**). The unenriched grafts displayed regions of branching NKX6.1$^+$/PDX1$^+$ pancreatic epithelial cells (**Fig. 4e**,**g**). Small clusters of NKX6.1$^+$/PDX1$^+$/insulin$^+$ cells resembling newly formed islets were detected amid this pancreatic epithelium, but not in the areas of the graft containing mainly polyhormonal cells. In contrast,

Table 1 CD142 immuno-magnetic cell separations of hES cell–derived pancreatic cultures

Cell line	Expt.	Marker	Pre-sort	Bound fraction	Flow-through fraction	Notes
CyT49	1	CD142^{bright}	55.5	90.2	33.9	a,b
		CHGA$^+$	36.1	8.29	49.8	
		CHGA$^-$/CD142^{bright}	47.1	86.0	26.1	
	2	CD142^{bright}	55.4	92.2	50.9	a
		CHGA$^+$	34.7	6.40	39.8	
		CHGA$^-$/CD142^{bright}	46.7	89.0	39.4	
	3	CD142^{bright}	58.8	92.9	56.3	a,c
		CHGA$^+$	20.7	4.04	19.5	
		CHGA$^-$/CD142^{bright}	55.3	90.3	53.1	
		CHGA$^-$/NKX6.1$^+$	56.9	86.5	51.4	
		CHGA$^-$/NKX6.1$^-$	22.4	9.46	29.1	
	4	CD142^{bright}	64.7	83.5	49.3	a,d
		CHGA$^+$	16.8	6.98	17.0	
		CHGA$^-$/CD142^{bright}	58.0	79.7	44.9	
		CHGA$^-$/NKX6.1$^+$	45.0	72.8	34.6	
		CHGA$^-$/NKX6.1$^-$	38.2	20.2	48.4	
	5	CD142^{bright}	45.6	94.7	45.1	e
		CHGA$^+$	24.3	4.31	23.4	
		CHGA$^-$/CD142^{bright}	41.6	91.5	40.1	
		CHGA$^-$/NKX6.1$^+$	37.1	85.6	33.9	
		CHGA$^-$/NKX6.1$^-$	38.6	10.1	42.7	
	6	CD142^{bright}	13.4	64.8	12.9	
		CHGA$^+$	7.76	6.50	7.80	
		CHGA$^-$/CD142^{bright}	12.9	61.6	12.3	
		CHGA$^-$/NKX6.1$^+$	6.60	48.7	5.72	
		CHGA$^-$/NKX6.1$^-$	85.6	44.8	86.5	
MEL1	7	CD142^{bright}	9.05	76.5	10.0	
		CHGA$^+$	0.33	0.98	0.44	
		CHGA$^-$/CD142^{bright}	8.98	75.7	9.98	
		CHGA$^-$/NKX6.1$^+$	1.87	39.2	0.13	
		CHGA$^-$/NKX6.1$^-$	96.8	59.9	99.3	
	8	CD142^{bright}	28.0	82.1	21.1	f
		CHGA$^+$	0.83	0.78	1.00	
		CHGA$^-$/CD142^{bright}	27.8	81.5	21.2	
		CHGA$^-$/NKX6.1$^+$	8.86	74.2	2.27	
		CHGA$^-$/NKX6.1$^-$	90.3	25.1	96.8	

Numbers reflect percentages of total intact cells in the population demarcated by the markers as determined by flow cytometry analyses.
(a) Cell material was transplanted into mice. (b) Additional data displayed in **Supplementary Figure 7b**. (c) Additional data displayed in **Figure 3a**. (d) Alternate machine sorting program was used. (e) Additional data displayed in **Supplementary Figure 7c**. (f) Additional data displayed in **Supplementary Figure 8c**. Expt., experiment; CHGA, chromogranin A.

CD318-enriched grafts exhibited only a few isolated groupings of NKX6.1$^+$/PDX1$^+$ cells scattered among weakly PDX1$^+$ cells, with no notable clusters of single-hormone insulin$^+$ cells (**Fig. 4f**,**h**). By 5 weeks after engraftment, larger groupings of single-hormone insulin$^+$ cells containing NKX6.1$^+$/PDX1$^+$ nuclei were obvious in the unenriched explants in proximity to regions of NKX6.1$^+$/PDX1$^+$ pancreatic epithelium (**Fig. 4m**). However, the CD318-enriched explants did not exhibit NKX6.1$^+$/PDX1$^+$ epithelium or NKX6.1$^+$/PDX1$^+$/insulin$^+$ cells (**Fig. 4n**). Notably, rather than principally polyhormonal cells, the CD318-enriched grafts now appeared to comprise many single-hormone glucagon$^+$ cells (**Fig. 4j**,**l**). In the unenriched explants, single-hormone glucagon$^+$ cells were also observed in areas that did and did not have the large insulin$^+$ clusters (**Fig. 4i**,**k**). After 9 weeks, mainly glucagon$^+$ cells were present in the CD318-enriched grafts along with a few scattered somatostatin$^+$ cells (**Fig. 4p**). As expected, the unenriched transplants contained large clusters of glucose-responsive insulin$^+$ cells in addition to other single-hormone glucagon$^+$ and somatostatin$^+$ endocrine cells[4] (**Fig. 4o**; data not shown).

Culturing of CD142-enriched PE cells

The formation of insulin$^+$ cell clusters in regions of branching epithelium in unenriched transplants, but not in endocrine-enriched transplants, suggested that islet progenitor potential resided in a nonendocrine (CHGA$^-$) population in pancreatic cultures. As the PE cells were prime candidates, we wanted to assess the developmental potential of transplanted CD142-enriched PE cells. However, our initial attempts to culture the CD142-enriched PE cells were unsuccessful. After dissociation, PE cells from unenriched or CD142-enriched cultures failed to aggregate, suggesting lack of survival or adhesion. This observation provided a potential explanation for the aforementioned enrichment of endocrine cells obtained by reaggregation of dissociated cultures. We examined the effect of the ROCK-inhibitor compound Y-27632 (ref. 11) upon aggregation of dissociated hES cell–derived pancreatic cultures (**Supplementary Fig. 7a**). In the absence of the compound, many CHGA$^+$, but few NKX6.1$^+$ cells, were detected in aggregates of unsorted cells. Inclusion of Y-27632 yielded aggregates containing large clusters of NKX6.1$^+$ cells in addition to CHGA$^+$ cells. The percentage of NKX6.1$^+$ cells, and more specifically PE cells, was similar before (40% NKX6.1$^+$; 37% CHGA$^-$/NKX6.1$^+$) and after (44% NKX6.1$^+$; 39% CHGA$^-$/NKX6.1$^+$) aggregation of nonsorted cells with Y-27632, arguing against induction of NKX6.1 expression by the compound in a large population of NKX6.1$^-$ cells.

Addition of Y-27632 allowed culturing of PE cells isolated by CD142 immuno-magnetic cell separation as well. The cellular composition of the CD142-bound fraction before (83% PE cells; 4% CHGA$^+$ cells) and after (89% PE cells; 4% CHGA$^+$ cells) aggregation with Y-27632 was similar, being enriched in PE cells and depleted in endocrine cells (**Supplementary Fig. 7c**). Immunofluorescence analyses showed that CD142-enriched PE aggregates from CyT49 cultures contained many NKX6.1$^+$/PDX1$^+$/CD142$^+$ cells, with pancreas transcription factor 1A (PTF1A) immunostaining of varying degrees of intensity (**Fig. 5a**). A few CHGA$^+$ cells were observed as well. Furthermore, qPCR analyses showed that CD142-enriched aggregates had higher expression of PE markers and lower expression of endocrine markers relative to nonsorted aggregates (**Supplementary Fig. 7b** and **Table 1**). CD142-enriched aggregates were similarly generated from MEL1 hES cell–derived pancreatic cultures, and these aggregates also displayed NKX6.1$^+$/PDX1$^+$/CD142$^+$ cells (**Supplementary Fig. 8b**). However, non-PE cells and CD142^{dim} cells were also present, as expected from the lower purities achieved in the bound fraction with this cell line (**Table 1** and **Supplementary Fig. 8a**). Finally, expression of PE markers was higher in CD142-bound aggregates and lower in CD142-flow-through aggregates compared with nonsorted aggregates, as assessed by qPCR (**Supplementary Fig. 8c**).

Developmental potential of PE cell–enriched population

Once culturing methods with Y-27632 were established for CD142-enriched PE cells, we performed four transplantation experiments with CD142-enriched material from four CyT49 cell separations (**Table 1**). In total, we transplanted eight mice with nonsorted aggregates from the pre-sort dissociated cell population, eight mice with CD142-enriched

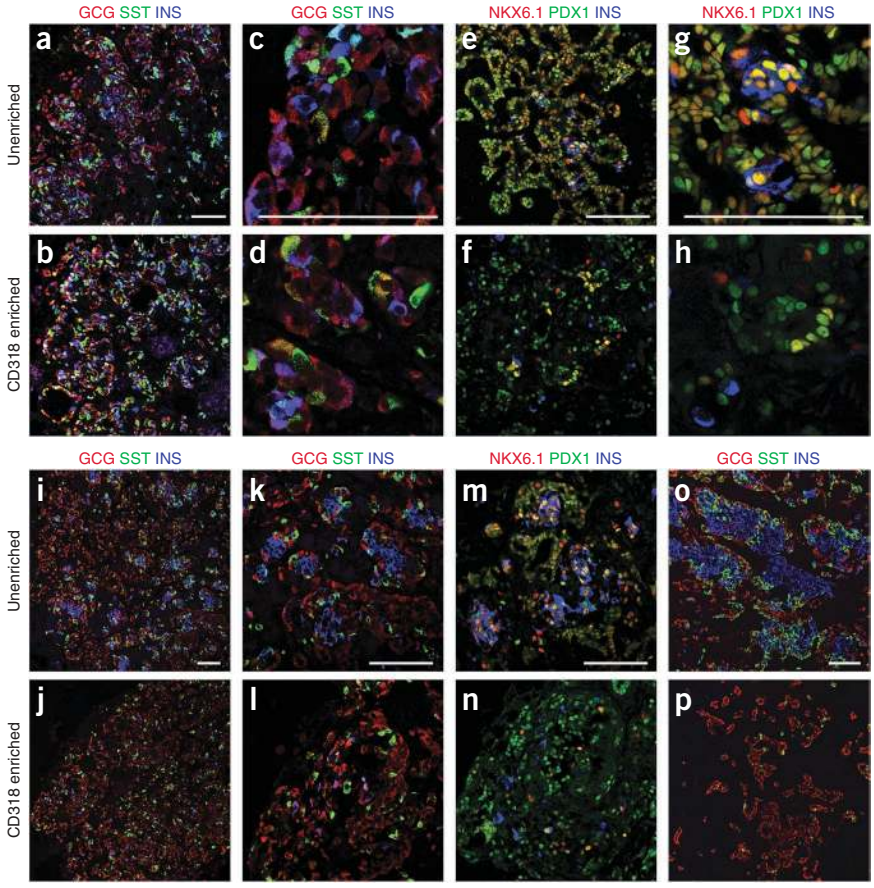

Figure 4 Immunofluorescence analyses of transplants of unenriched or CD318-enriched endocrine cells. (**a**–**h**) Grafts at 3 weeks after transplant. Unenriched (**a**,**c**,**e**,**g**) and CD318-enriched (**b**,**d**,**f**,**h**) explants stained with (**a**–**d**) anti-GCG (red), anti-SST (green), anti-INS (blue) or (**e**–**h**) anti-NKX6.1 (red), anti-PDX1 (green) and anti-INS (blue). (**i**–**n**) Grafts at 5 weeks after transplant. Unenriched (**i**,**k**,**m**) or CD318-enriched (**j**,**l**,**n**) explants stained with (**i**–**l**) anti-GCG (red), anti-SST (green), anti-INS (blue) or (**m**,**n**) anti-NKX6.1 (red), anti-PDX1 (green), anti-INS (blue). (**o**,**p**) Unenriched graft at 19 weeks after transplant (**o**) or CD318-enriched graft at 9 weeks after transplant (**p**) stained with anti-GCG (red), anti-SST (green) and anti-INS (blue). The CD318-enriched transplanted cells were enriched in endocrine cells and depleted in PE cells (**Supplementary Table 1**, experiment 7). Scale bars, 100 μm. INS, insulin; GCG, glucagon; SST, somatostatin.

aggregates from the bound fraction and four mice with intact aggregates generated with a tissue chopper from nondissociated cultures. All three types of transplanted aggregates gave rise to functional, glucose-responsive, insulin-secreting cells *in vivo* (nonsorted 100%; CD142-enriched 50%; intact 100%), as measured by levels of human C-peptide in mouse sera before and after glucose administration (**Fig. 5b** and data not shown). Four mice with CD142-enriched glucose-responsive grafts came from three separate experiments (**Table 1**, experiments 1–3). In three of the CD142-enriched animals lacking functional grafts, no engrafted tissue was found. An additional mouse had a small CD142-enriched graft that secreted lower levels of human C-peptide (**Fig. 5b**, mouse number 4). Explants of unenriched material (intact and nonsorted aggregates) in the four separate experiments exhibited teratomous graft rates of 25% (expt. 1, $n = 1/4$), 0% (expt. 2, $n = 0/8$), 67% (expt. 3, $n = 4/6$) and 100% (expt. 4, $n = 6/6$). However, none of the seven surviving CD142-enriched grafts from experiments 1–3 were teratomous.

CD142-enriched explants exhibited islet-like clusters of NKX6.1$^+$/PDX1$^+$/insulin$^+$ cells surrounded by somatostatin$^+$ and glucagon$^+$ cells, similar to unenriched explants (**Fig. 5c**–**f**). As observed with unenriched cells, CD142-enriched transplants also gave rise to other PE progenitor lineages including PTF1A$^+$/trypsin$^+$ exocrine cells (**Fig. 5g**,**h**) and PDX1$^+$/CK19$^+$ ductal cells (**Fig. 5i**,**j**). The CK19$^+$ and somatostatin$^+$ cells appeared to have weaker PDX1$^+$ nuclear staining compared with the large PDX1$^+$/insulin$^+$ clusters. These data show that CD142-enriched PE cells have the potential to generate all three pancreatic lineages, including functional insulin cells, *in vivo*.

DISCUSSION

We have identified cell-surface markers that will serve as valuable tools for analyses of pancreatic cell subsets in stem cell–derived cultures. Both CD200 (encoded by *OX-2*), a member of the immunoglobulin superfamily, and CD318 (encoded by *CDCP1*), a CUB domain–containing protein, have been reported to be expressed in the human adult pancreas (http://www.proteinatlas.org/)[12,13]. Expression of CD142 (encoded by *F3*) has been described in the human fetal pancreas in early pancreatic epithelium at 8 weeks and later in the acini[14]. Notably, CD142 (tissue factor), which forms a complex with Factor VII/VIIa to initiate blood coagulation, has been shown to participate in the instant blood-mediated inflammatory reaction associated with poor engraftment and intraportal thrombosis after islet transplantation in the liver owing to its expression in human islet preparations[15,16].

Our hES cell–derived cultures comprise a mixture of cell types, including PE cells and polyhormonal endocrine cells. Studies of mouse pancreas development have demonstrated that beta cells arise from pancreatic progenitors and not from the primary endocrine cells, an early born endocrine population that that does not substantially contribute to the adult pancreas and differs in several respects from mature endocrine cells, including polyhormonal expression[1,8,17–21]. Previously, we proposed a similar hypothesis to explain the origin of the functional beta cells we observed after transplantation[4]. The identification of the cell-surface markers described here enabled us to test this hypothesis and demonstrate that populations enriched in PE cells gave rise to functional beta cells but that populations enriched in polyhormonal cells did not. We cannot exclude the possibility that the endocrine cells have the potential to give rise to beta cells but only in the presence of PE cells, such that upon separation of these populations the activity is lost. Although we did not further analyze the eventual fate and function of the polyhormonal cells, a recent study described transplantation of hES cell–derived polyhormonal cells that similarly appeared to resolve into glucagon$^+$ cells, which were functional[22]. It has recently been shown that alpha cells can convert to beta cells in mice after either ablation of beta cells or overexpression of Pax4 in glucagon cells[23–25]. It would be intriguing to assess whether hES cell–derived polyhormonal endocrine cells also have the potential to give rise to beta cells under these conditions or in other circumstances requiring beta cell regeneration.

In contrast to the polyhormonal cells, enriched PE cells did yield islet-like clusters and ductal and exocrine tissue after implantation.

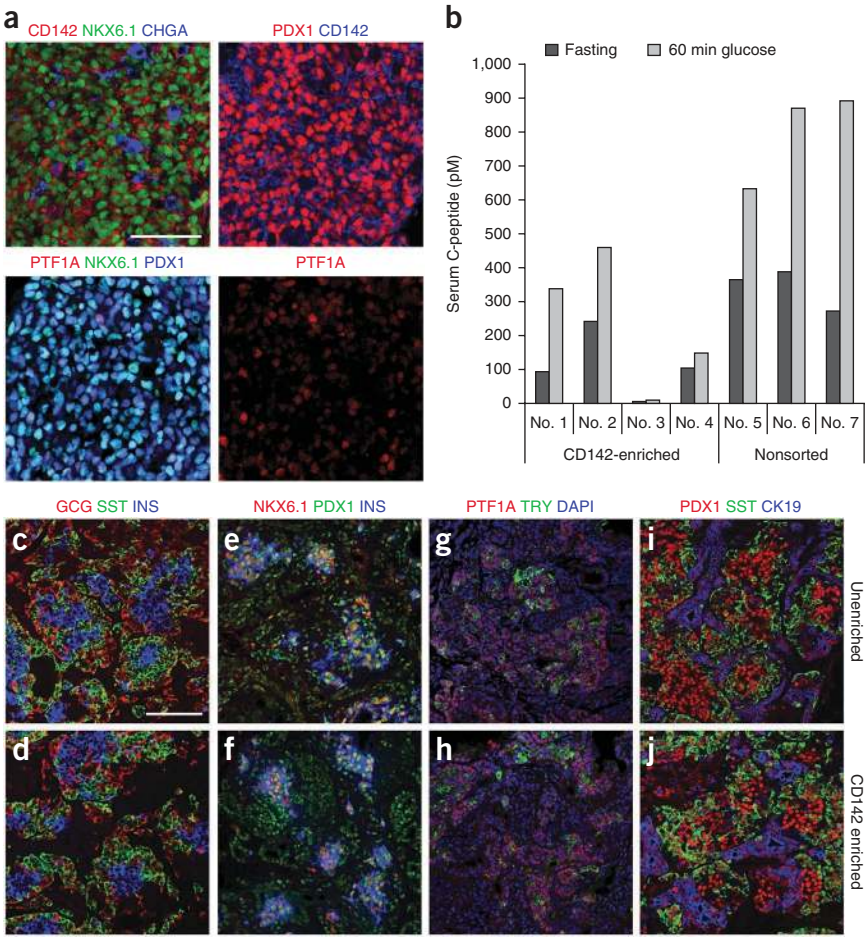

Figure 5 Immunofluorescence and functional analyses of transplants of unenriched or CD142-enriched PE cells. (**a**) CD142-enriched cellular aggregates cultured in the presence of Y-27632 (10 μM) were stained with anti-NKX6.1 (green), anti-PDX1 (red, blue), anti-CD142 (red, blue), anti-CHGA (blue) and anti-PTF1A (red). Scale bar, 50 μm. (**b**) Analyses of human C-peptide levels in mouse sera after fasting and 60 min after glucose injection 10 weeks after transplant. Mice were transplanted with CD142-enriched cells and nonsorted cells that were aggregated with Y-27632 (10 μM). The transplanted CD142-enriched cells were enriched in PE cells and depleted in endocrine cells (**Table 1** and **Supplementary Fig. 7**). (**c**–**j**) Grafts at 13 weeks after transplant. Unenriched (**c**,**e**,**g**,**i**) and CD142-enriched grafts (**d**,**f**,**h**,**j**) stained with (**c**,**d**) anti-GCG (red), anti-SST (green), anti-INS (blue) (**e**,**f**) anti-NKX6.1 (red), anti-PDX1 (green), anti-INS (blue) (**g**,**h**) anti-PTF1A (red), anti-TRY (green), DAPI (blue) (**i**,**j**) anti-PDX1 (red), anti-SST (green) and anti-CK19 (blue). Scale bar, 100 μm. INS, insulin; GCG, glucagon; SST, somatostatin; TRY, trypsin; No., mouse number.

Hence, CD142-enriched PE cells, which are PDX1^{+}/NKX6.1^{+}/PTF1A^{+}[26], are multipotent pancreatic progenitors that can generate all three pancreatic lineages. Because the transplanted populations were not enriched to purity, it is formally possible that a minor contaminating cell type had the progenitor potential instead. This hypothesis seems less likely given that the contaminating cells were polyhormonal cells and unidentified cells and that PE cells are known to be pancreatic progenitors during development. Also, we have more recently obtained functional insulin-secreting cells from transplanted populations that were more enriched in CD142^{bright} cells and PE cells (respectively, 98% and 93%; data not shown). Even so, the presence of other cell types may support the engraftment and survival of PE progenitors, an idea consistent with the observation that engrafted tissue was not found for 5 out of 12 of the CD142-enriched grafts. As we did not assess the developmental potential of nonendocrine (CHGA^{-}) cell types in the CD142^{dim} population, we cannot exclude the possibility that they may have some progenitor potential as well, especially considering that PE cells were present in variable proportions in the CD142^{dim} fraction. The difference between these two distinct PE populations is unclear.

Another advance of this work was the discovery that inclusion of the ROCK-inhibitor compound, Y-27632, allowed for the recovery of cellular aggregates containing PE progenitors from dissociated cultures, as has been shown for undifferentiated hES cells and hES cell–derived cardiomyocytes[11,27]. The underlying mechanism is unclear; Y-27632 may improve survival, possibly by preventing anoikis, and/or it may enhance cell-cell interactions for aggregation[5,28,29]. Regardless of the mechanism, cultures enriched in PE cell progenitors could allow for screening of molecules and cell types that induce their differentiation, survival and proliferation. The ability of CD142-enriched PE cell progenitors to generate pancreatic lineages *in vivo* demonstrates the utility of these cells as suitable starting material for many investigations.

It will be critical to examine the specificity of these surface markers in other systems. The fact that both CD200 and CD318 showed similar staining patterns in cultures derived from multiple hES cell lines, as well as being localized in adult islets, suggests they should be generally useful for assessment of endocrine cells, with CD200 exhibiting greater specificity for endocrine cells than CD318. CD142 intensity increased after the onset of expression of NKX6.1 protein, making CD142 a marker principally for NKX6.1^{+}/PDX1^{+} PE cell progenitors. Although the CD142^{bright} population was not exclusively composed of PE cells, there was a positive correlation between the number of CD142^{bright} cells and the number of PE cells in pancreatic cultures. However, in cultures not treated with keratinocyte growth factor (KGF) at stage 2, which were evaluated in the antibody screen, a population of CD142^{bright} cells was detected largely in the absence of PE cells (**Supplementary Fig. 9**). The identity of this population is unknown, but is not unexpected given that CD142 has been described in other cell types during human development[14]. Nonetheless, CD142 was able to distinguish and enrich PE cells in pancreatic cultures derived from multiple hES cell lines, suggesting that CD142 should have broad utility for analyses of PE in pluripotent stem cell–derived cultures. We note that CD24 was recently reported to be a PDX1^{+} pancreatic progenitor marker after human ES cell differentiation[30]. We observed that CD24 exhibited a rather widespread expression pattern in our antibody screen, a difference yet to be investigated. It will be interesting to determine whether CD142, CD200 and CD318 might also be useful for isolating pancreatic cell subsets from human tissues at adult and fetal stages. Likewise, it will be interesting to assess in our hES cell–derived pancreatic cultures the dynamics of expression of cell-surface antibodies identified for adult

and fetal pancreatic tissues[31–33]. One of these markers, the pan-islet marker HPi3 (ref. 31), has been shown to enrich for hormone-expressing cells from differentiated hES cultures[34].

An important concern in the development of hES cell–derived cell therapies is the potential for the formation of teratomas. In our previous publication with transplants of unenriched pancreatic cultures, some of the grafts (15%) were teratomous[4]. Of the four CD142 enrichment transplant experiments performed in the present study, 11 of the 24 (46%) unenriched grafts were teratomous. However, all but one of the teratomous grafts came from only two of the four experiments, suggesting some degree of experimental variability. No teratomous grafts were observed in the seven surviving CD142-enriched grafts, supporting the idea that enrichment of PE cells can reduce the probability of teratoma formation. However, definitive statements about the absence of teratoma formation upon enrichment would require assessment of more grafts from additional experiments given that in some experiments few teratomas were observed even from unpurified grafts and that some of the CD142-enriched transplants failed to engraft and/or survive.

For a diabetes cell therapy, dose estimates projected from human islet transplantations are very high—on the order of 100 million cells. During cell separation, a considerable loss of target cells was observed, suggesting that substantially more cells could be required during manufacturing for a process that involves a cell enrichment step. Although purification methods could possibly be improved to increase recovery, we have focused on developing protocols that allow for more consistent and efficient production of pancreatic cells derived from hES cells, thereby obviating the need for cell purification. This optimization has been greatly aided by the discovery of cell-surface markers for monitoring pancreatic differentiation.

METHODS

Methods and any associated references are available in the online version of the paper at http://www.nature.com/naturebiotechnology/.

Note: Supplementary information is available on the Nature Biotechnology website.

ACKNOWLEDGMENTS

We thank O. Madsen (Hagedorn Research Institute), C. Wright (Vanderbilt University), J. Johnson (UT Southwestern Medical Center) and BD Biosciences for providing antibodies and A. Elefanty and E. Stanley (Monash University) for providing the MEL1 hES cell line. The CyT203 and CyT49 hES cell lines were derived with partial funding from the Juvenile Diabetes Research Foundation.

AUTHOR CONTRIBUTIONS

O.G.K. and A.G.B. wrote the paper. O.G.K. and A.G.B. designed, directed and interpreted experiments with intellectual contributions from E.E.B., M.M., L.A.M., E.K., K.A.D., K.K. and M.K.C. The antibody screen was proposed by A.G.B. and carried out by O.G.K., M.Y.C. and M.M. K.A.D. suggested the Y-27632 compound. M.M. developed and performed the flow cytometry assays and analyses with assistance from M.Y.C. and K.G.R. O.G.K., A.G.B., M.Y.C. and T.M.O. performed the cell culture experiments and immuno-magnetic cell separations. M.Y.C. and O.G.K. performed qPCR and immunofluorescence analyses of *in vitro* material. L.A.M., E.K. and M.R. executed the *in vivo* experiments, including transplantations and C-peptide assays. K.K. performed the histological and immunofluorescence analyses of implanted grafts.

COMPETING FINANCIAL INTERESTS

The authors declare competing financial interests: details accompany the full-text HTML version of the paper at http://www.nature.com/nbt/index.html.

Published online at http://www.nature.com/nbt/index.html.
Reprints and permissions information is available online at http://www.nature.com/reprints/index.html.

1. Guo, T. & Hebrok, M. Stem cells to pancreatic beta-cells: new sources for diabetes cell therapy. *Endocr. Rev.* **30**, 214–227 (2009).
2. Van Hoof, D., D'Amour, K.A. & German, M.S. Derivation of insulin-producing cells from human embryonic stem cells. *Stem Cell Res. (Amst.)* **3**, 73–87 (2009).
3. D'Amour, K.A. *et al.* Production of pancreatic hormone-expressing endocrine cells from human embryonic stem cells. *Nat. Biotechnol.* **24**, 1392–1401 (2006).
4. Kroon, E. *et al.* Pancreatic endoderm derived from human embryonic stem cells generates glucose-responsive insulin-secreting cells *in vivo*. *Nat. Biotechnol.* **26**, 443–452 (2008).
5. Sugiyama, T. & Kim, S.K. Fluorescence-activated cell sorting purification of pancreatic progenitor cells. *Diabetes Obes. Metab.* **10** (suppl. 4), 179–185 (2008).
6. McKnight, K.D., Wang, P. & Kim, S.K. Deconstructing pancreas development to reconstruct human islets from pluripotent stem cells. *Cell Stem Cell* **6**, 300–308 (2010).
7. Winkler, H. & Fischer-Colbrie, R. The chromogranins A and B: the first 25 years and future perspectives. *Neuroscience* **49**, 497–528 (1992).
8. Pan, F.C. & Wright, C. Pancreas organogenesis: from bud to plexus to gland. *Dev. Dyn.* **240**, 530–565 (2011).
9. Murray, H.E., Paget, M.B. & Downing, R. Preservation of glucose responsiveness in human islets maintained in a rotational cell culture system. *Mol. Cell. Endocrinol.* **238**, 39–49 (2005).
10. Gao, R., Ustinov, J., Korsgren, O. & Otonkoski, T. In vitro neogenesis of human islets reflects the plasticity of differentiated human pancreatic cells. *Diabetologia* **48**, 2296–2304 (2005).
11. Watanabe, K. *et al.* A ROCK inhibitor permits survival of dissociated human embryonic stem cells. *Nat. Biotechnol.* **25**, 681–686 (2007).
12. Miyazawa, Y. *et al.* CUB domain-containing protein 1, a prognostic factor for human pancreatic cancers, promotes cell migration and extracellular matrix degradation. *Cancer Res.* **70**, 5136–5146 (2010).
13. Uhlen, M. *et al.* Towards a knowledge-based Human Protein Atlas. *Nat. Biotechnol.* **28**, 1248–1250 (2010).
14. Luther, T. *et al.* Tissue factor expression during human and mouse development. *Am. J. Pathol.* **149**, 101–113 (1996).
15. Moberg, L. *et al.* Production of tissue factor by pancreatic islet cells as a trigger of detrimental thrombotic reactions in clinical islet transplantation. *Lancet* **360**, 2039–2045 (2002).
16. Beuneu, C. *et al.* Human pancreatic duct cells exert tissue factor-dependent procoagulant activity: relevance to islet transplantation. *Diabetes* **53**, 1407–1411 (2004).
17. Gu, G., Dubauskaite, J. & Melton, D.A. Direct evidence for the pancreatic lineage: NGN3$^+$ cells are islet progenitors and are distinct from duct progenitors. *Development* **129**, 2447–2457 (2002).
18. Kawaguchi, Y. *et al.* The role of the transcriptional regulator Ptf1a in converting intestinal to pancreatic progenitors. *Nat. Genet.* **32**, 128–134 (2002).
19. Teitelman, G., Alpert, S., Polak, J.M., Martinez, A. & Hanahan, D. Precursor cells of mouse endocrine pancreas coexpress insulin, glucagon and the neuronal proteins tyrosine hydroxylase and neuropeptide Y, but not pancreatic polypeptide. *Development* **118**, 1031–1039 (1993).
20. Herrera, P.L. Adult insulin- and glucagon-producing cells differentiate from two independent cell lineages. *Development* **127**, 2317–2322 (2000).
21. Wilson, M.E., Kalamaras, J.A. & German, M.S. Expression pattern of IAPP and prohormone convertase 1/3 reveals a distinctive set of endocrine cells in the embryonic pancreas. *Mech. Dev.* **115**, 171–176 (2002).
22. Rezania, A. *et al.* Production of functional glucagon-secreting alpha cells from human embryonic stem cells. *Diabetes* **60**, 239–247 (2011).
23. Collombat, P. *et al.* The ectopic expression of Pax4 in the mouse pancreas converts progenitor cells into alpha and subsequently beta cells. *Cell* **138**, 449–462 (2009).
24. Thorel, F. *et al.* Conversion of adult pancreatic alpha-cells to beta-cells after extreme beta-cell loss. *Nature* **464**, 1149–1154 (2010).
25. Chung, C.H., Hao, E., Piran, R., Keinan, E. & Levine, F. Pancreatic beta-cell neogenesis by direct conversion from mature alpha-cells. *Stem Cells* **28**, 1630–1638 (2010).
26. Hald, J. *et al.* Generation and characterization of Ptf1a antiserum and localization of Ptf1a in relation to Nkx6.1 and Pdx1 during the earliest stages of mouse pancreas development. *J. Histochem. Cytochem.* **56**, 587–595 (2008).
27. Braam, S.R., Nauw, R., Ward-van Oostwaard, D., Mummery, C. & Passier, R. Inhibition of ROCK improves survival of human embryonic stem cell-derived cardiomyocytes after dissociation. *Ann. NY Acad. Sci.* **1188**, 52–57 (2010).
28. Koyanagi, M. *et al.* Inhibition of the Rho/ROCK pathway reduces apoptosis during transplantation of embryonic stem cell-derived neural precursors. *J. Neurosci. Res.* **86**, 270–280 (2008).
29. Krawetz, R.J., Li, X. & Rancourt, D.E. Human embryonic stem cells: caught between a ROCK inhibitor and a hard place. *Bioessays* **31**, 336–343 (2009).
30. Jiang, W. *et al.* CD24: a novel surface marker for PDX1-positive pancreatic progenitors derived from human embryonic stem cells. *Stem Cells* **29**, 609–617 (2011).
31. Dorrell, C. *et al.* Isolation of major pancreatic cell types and long-term culture-initiating cells using novel human surface markers. *Stem Cell Res. (Amst.)* **1**, 183–194 (2008).
32. Sugiyama, T., Rodriguez, R.T., McLean, G.W. & Kim, S.K. Conserved markers of fetal pancreatic epithelium permit prospective isolation of islet progenitor cells by FACS. *Proc. Natl. Acad. Sci. USA* **104**, 175–180 (2007).
33. Hori, Y., Fukumoto, M. & Kuroda, Y. Enrichment of putative pancreatic progenitor cells from mice by sorting for prominin1 (CD133) and platelet-derived growth factor receptor beta. *Stem Cells* **26**, 2912–2920 (2008).
34. Nostro, M.C. *et al.* Stage-specific signaling through TGFbeta family members and WNT regulates patterning and pancreatic specification of human pluripotent stem cells. *Development* **138**, 861–871 (2011).

ONLINE METHODS

Animal care. All experiments and procedures were approved by the Institutional Care and Use Committee.

hES cell culture and differentiation. CyT49, CyT203 and MEL1 hES cells were maintained as previously described in 60-mm tissue culture plates[3]. Cultures were either manually passaged or enzymatically passaged with dispase (Invitrogen) or accutase (Innovative Cell Technologies) at 1:4 to1:10 split ratios every 3–7 d. Karyotype analysis using the G-banding technique was routinely performed on hES cell cultures (Children's Hospital Oakland). For most of the experiments, pancreatic differentiation was done as previously described[3,4] (**Supplementary Fig. 1a**) with the following minor modifications: (i) on the first day of stage 1 the concentration of mouse Wnt3A (R&D Systems) was increased to 50 ng/ml; (ii) on the first day of stage 2 sometimes either 5 μM SB431542 (Sigma) or 2.5 μM TGFβ inhibitor IV (EMD Bioscience) was also included; (iii) during stage 3 the concentration of retinoic acid (BIOMOL) was decreased to 1 μM; (iv) during stages 4 and 5, cultures were maintained in DMEM (HyClone) media containing 1% (vol/vol) B27 (Invitrogen) until cells were processed or analyzed. For the antibody screening shown in **Supplementary Figure 2**, the CyT49 hES cell–derived pancreatic cultures were differentiated using a slightly modified stage 3 step that entailed culturing for 1 d with 0.2 μM retinoic acid and 0.25 μM KAAD-cyclopamine (Toronto Research Chemicals) followed by 4 d with 30 ng/ml Noggin (R&D Systems). All media were supplemented with GlutaMAX and penicillin/streptomycin from Invitrogen.

Flow cytometry. For the initial screen 217 purified antibodies (0.5 μg/test) to cell-surface antigens were examined (BD Biosciences, Biolegend) in conjunction with the appropriate fluorochrome-conjugated secondary antibodies. The purified antibodies from BD Biosciences were provided as a generous gift. Subsequent surface marker analyses were performed with the following fluorochrome-conjugated antibodies (1:10 dilution chosen after titration analyses): CD56-PE BD (no. 340363), CD142-PE (BD no. 550312), CD200-PE (BD no. 552475), CD200-APC (R&D Systems no. FAB27241A), CD318-PE (Biolegend no. 324006). Plates of hES cell–derived pancreatic cultures were washed in PBS and then enzymatically dissociated to single-cell suspension using either TrypLE (Invitrogen) or Accumax (Innovative Cell Technologies) at 37 °C. FBS buffer (PBS, 3% (vol/vol) FBS) was added and the suspension was passed through a 40–100 μm filter, pelleted and resuspended in FBS buffer at ~1×10^7 cells/ml. Cells were incubated with surface marker antibody for 15–30 min at ~4 °C–25 °C. Cells were washed in FBS buffer and then similarly processed with secondary antibody when needed. After staining, cells were fixed for 30 min in 4% (wt/vol) paraformaldehyde. Cells were washed in FBS buffer and stored in IC Buffer (PBS, 1% (wt/vol) BSA, 0.1% (wt/vol) NaN_3) for subsequent intracellular staining.

For intracellular staining the following primary antibodies were used: goat anti-PDX1 (Abcam no. ab47383; gift from Chris Wright), mouse anti-NKX6.1 (Developmental Studies Hybridoma Bank no. F55A12), rabbit anti-chromogranin A (DAKO no. A0430). When co-staining with other mouse antibodies, the mouse anti-NKX6.1 antibody was directly conjugated to the fluorochrome Alexa488 using the Zenon kit (Invitrogen). Secondary antibodies were obtained from Jackson Immunoresearch, Invitrogen and BD Biosciences. Cells were permeabilized with Perm Buffer (PBS, 0.2% (wt/vol) Triton X-100, 5% (vol/vol) normal donkey serum, 0.1% (wt/vol) NaN_3) for 30 min on ice then washed with IC buffer. Cells were incubated with primary antibodies diluted with Block Buffer (PBS, 0.1% (wt/vol) Triton X-100, 5% (vol/vol) normal donkey serum, 0.1% (wt/vol) NaN_3) overnight at 4 °C. Cells were washed in IC buffer and then incubated with appropriate secondary antibodies for 60 min at 4 °C. Cells were washed with IC Buffer and then in FACS Buffer. Cells were resuspended in FACS buffer (PBS, 0.1% (wt/vol) BSA, 0.1% (wt/vol) NaN_3) for flow acquisition.

Flow cytometry data was acquired with a FACSCalibur (BD Biosciences), using excitation lines at 488 nm and 635 nm and detecting fluorescence at 530 ± 15 nm, 585 ± 21 nm and 661 ± 8 nm. Data were analyzed using FlowJo software (Tree Star). Intact cells were identified based on forward (low angle) and side (orthogonal, 90°) light scatter, and subsequently, analyzed for fluorescence intensity. In some cases, additional gating of intact cells (populations 1–3) was performed to account for the varying levels of autofluorescence observed in these complex samples. Background was estimated using unstained, secondary antibody alone, or irrelevant antibody controls, as appropriate. A gating scheme is displayed in **Supplementary Figure 3**. In most figures a representative flow cytometry plot is shown from either population 1 or population 2 with numbers presented on the plots indicating the percentage of total cells from the intact cells gate. In populations containing low percentages of endocrine cells the anti-chromogranin A antibody stains with greater intensity. We have seen a similar pattern with hormone staining as well[3].

Cell sorting. Cell sorting was performed using MACS cell separation technology and reagents from Miltenyi Biotec. Direct magnetic labeling was performed using CD56 microbeads and indirect magnetic labeling was performed using anti-PE microbeads with one of the following PE-conjugated antibodies: CD142-PE, CD200-PE or CD318-PE. Cell separation was performed substantially according to the manufacturer's instructions although cells were typically resuspended in a larger volume before loading on the separation column. Sorting buffer used for antibody staining, washing and cell separation was either PBS with 3% (vol/vol) FBS and 1 mM EDTA or PBS with 0.5% (wt/vol) BSA and 2 mM EDTA. For CD142 separations 10 μM Y-27632 (Alexis Biochemicals) was sometimes included in the sorting buffer. Cells were dissociated to single-cell suspensions as described in the flow cytometry section. Cell separations were performed using either a manual system with LS MACS cell separation columns on a QuadroMACS Separation Unit or an automated system with the autoMACS Pro Separator. Briefly, cells were loaded on the column while attached to the magnet, and after several washes, cells were collected in buffer as the flow-through fraction. Then the column was removed from the magnet and the cells remaining on the column were eluted as the bound fraction. The cell fractions were either cultured or fixed for flow cytometry analyses. Alternatively, cell sorting was performed with FACS using a BD FACSAria with the same sorting buffers and PE-conjugated antibodies.

Culture of cell aggregates. Reaggregation of dispersed cells was done with rotational culture. Enzymatically dissociated cultures were placed in six-well ultra-low attachment plates (Costar) at a concentration of ~1×10^6 cells/ml in a volume of 6 ml. The six-well plate was placed on a platform shaker (VWR) at a speed of 100 r.p.m. and cellular aggregates formed overnight. Aggregation was performed in DMEM (Hyclone) with 1–2% (vol/vol) FBS, 1% (vol/vol) B27 supplement (Invitrogen) and 25–50 μg/ml DNase. In some cases a caspase inhibitor (5–10 μM Z-VAD-FMK; R&D systems) was also included. DNase and the caspase inhibitor were removed from the media the following day. For endocrine enrichment, with or without prior antibody immuno-magnetic selection, Y-27632 (Alexis) was omitted. Otherwise Y-27632 (10–15 μM) was included upon aggregation of unenriched or CD142-enriched cells. Both components were removed from the media the following day. CD142-enriched cells had a tendency to form large aggregates so in some cases aggregation in rotational culture was performed for 4–6 h and the cell clusters were then loaded on Gelfoam for further culture. Alternatively, CD142-enriched cells were cultured in 24-well ultra-low attachment plates overnight in static culture. The next day thin multilayered cell discs had formed.

Immunofluorescence. Differentiated hES cell–derived aggregates and graft explants were fixed and processed for cryosectioning as previously described[4]. Immunofluorescence analyses of cryosections and intact plate cultures were performed as previously described[3,4]. The following primary antibodies were used: rabbit anti-chromogranin A (DAKO no. A0430), guinea pig anti-insulin (Dako no. A0564), rabbit anti-somatostatin (DAKO no. A0566), goat anti-somatostatin (Santa Cruz no. SC7819), mouse anti-glucagon (Sigma no. G2654), rabbit anti-glucagon (Invitrogen no. 18-0064), guinea pig anti-PDX1 (Abcam no. ab7308), goat anti-PDX1 (Abcam no. ab47383), goat anti-PDX1 (gift from C. Wright), rabbit anti-NKX6.1 (gift from O. Madsen), guinea pig anti-PTF1A (purchased from UT Southwestern Medical Center), rabbit anti-trypsin (Biodesign no. K50900R), rabbit anti-CK19 (Abcam no. ab52907), goat anti-CD142 (R&D Systems no. AF2339), goat anti-CD200 (R&D systems no. AF2724), goat anti-CD318 (R&D systems no. AF2666) and mouse anti-NKX6.1 (Developmental Studies Hybridoma Bank no. F55A12) that was directly conjugated to Alexa555 fluorochrome using the APEX antibody labeling kit (Invitrogen). Vectashield (Vector Labs) mounting medium was used.

Immunofluorescence imaging was performed at 25 °C using a Nikon C1-Plus Confocal Microscope (Nikon) equipped with 10× Plan Apo (Nikon, WD = 4.0 mm, NA = 0.45), 20× Plan Apo (Nikon, WD = 1.0 mm, NA = 0.75), 40× Plan Apo (Nikon, WD = 0.14 mm, NA = 0.95), and 20× Fluor (Nikon, WD = 2.0 mm, NA = 0.50W) objectives, an acousto-optic tunable filter, and solid state laser lines at 408 nm (17 mW), 488 nm (50 mW), 561 nm (10 mW) and 638 nm (10 mW). Descanned emission from fluorophores was filtered through the primary quad band mirror (z405/488/561/638rpc, Chroma Technology) then detected by three photomultiplier tubes on four channels using a dual dichroic beamsplitter that reflects at 408/638 nm to a dual emission filter transmitting at 408/638 nm, and a 560 nm long-pass dichroic mirror that reflects to a 525/50 nm bandpass filter or transmits to a 595/50 nm bandpass filter. The dwell time and pinhole diameter for all image scans were 1.68 µsec and 30 µm, respectively. Digital images were acquired using Nikon EZ-C1 Acquisition software (Nikon) at 16 bits and 1,024 × 1,024 pixel resolution, with final images created by frame averaging three duplicate images. Laser intensity and gain were adjusted to prevent pixel saturation. Digital processing of images was performed using Adobe Photoshop. Manipulations included cropping a portion of an image from a larger field and changing brightness and contrast. Adjustments were performed on the entire image and equally on experimental conditions. In **Figure 5e–h** color channels were individually adjusted for better visualization of the data in the merged image.

Quantitative PCR. Real-time PCR was done using methods and primer sequences as previously described[3,4]. Duplicate cell samples were taken for RNA extraction and PCR reactions were run in duplicate or triplicate. Relative quantification was performed against a standard curve and quantified values for a gene of interest were normalized to input of two housekeeping genes (*CYCG* and *TBP*). The data are represented as the mean and the s.d. of four to six gene expression measurements with similar observations made in at least two independent experiments. For statistical analysis an unpaired *t*-test was used.

Implant preparation. A minor modification from our previous publication[4] was that aggregates generated with a tissue chopper were incubated in six-well ultra-low attachment plates in rotational culture in media containing DNase (25–50 µg/ml). Cellular aggregates generated with a tissue chopper or aggregation in rotational culture were allowed to settle by gravity and loaded on to Gelfoam discs, as previously described[4]. CD142-enriched cells that were incubated in static culture were cut into pieces and loaded on a Gelfoam disc.

Transplantation and glucose-stimulated insulin secretion. Transplants into severe combined immunodeficient–beige mice and subsequent analyses of graft function were performed essentially as described[4]. Briefly, implant constructs of Gelfoam loaded with cells were placed in the epididymal fat pad. Approximately 2 to 6×10^6 cells were transplanted into each mouse. Enzyme-linked immunosorbent assays (Mercodia) were used to measure sera levels of human c-peptide before and 60 min after administration of glucose to mice that had been fasted for ~20 h.

doi:10.1038/nbt.1931